Granulometry-Based Trabecular Bone Segmentation

Manish Chowdhury[1], Benjamin Klintström[1,2], Eva Klintström[2], Örjan Smedby[1,2], and Rodrigo Moreno[1(✉)]

[1] KTH, School of Technology and Health, Hälsovägen 11c, 14157 Huddinge, Sweden
{manish.chowdhury,orjan.smedby,rodrigo.moreno}@sth.kth.se, benklint@gmail.com

[2] Center for Medical Image Science and Visualization, Linköping University, Linköping, Sweden
evaklintstrom@gmail.com

Abstract. The accuracy of the analyses for studying the three dimensional trabecular bone microstructure rely on the quality of the segmentation between trabecular bone and bone marrow. Such segmentation is challenging for images from computed tomography modalities that can be used in vivo due to their low contrast and resolution. For this purpose, we propose in this paper a granulometry-based segmentation method. In a first step, the trabecular thickness is estimated by using the granulometry in gray scale, which is generated by applying the opening morphological operation with ball-shaped structuring elements of different diameters. This process mimics the traditional sphere-fitting method used for estimating trabecular thickness in segmented images. The residual obtained after computing the granulometry is compared to the original gray scale value in order to obtain a measurement of how likely a voxel belongs to trabecular bone. A threshold is applied to obtain the final segmentation. Six histomorphometric parameters were computed on 14 segmented bone specimens imaged with cone-beam computed tomography (CBCT), considering micro-computed tomography (micro-CT) as the ground truth. Otsu's thresholding and Automated Region Growing (ARG) segmentation methods were used for comparison. For three parameters (Tb.N, Tb.Th and BV/TV), the proposed segmentation algorithm yielded the highest correlations with micro-CT, while for the remaining three (Tb.Nd, Tb.Tm and Tb.Sp), its performance was comparable to ARG. The method also yielded the strongest average correlation (0.89). When Tb.Th was computed directly from the gray scale images, the correlation was superior to the binary-based methods. The results suggest that the proposed algorithm can be used for studying trabecular bone in vivo through CBCT.

Keywords: Cone beam computed tomography · Segmentation · Granulometry · Trabecular bone

© Springer International Publishing AG 2017
P. Sharma and F.M. Bianchi (Eds.): SCIA 2017, Part II, LNCS 10270, pp. 100–108, 2017.
DOI: 10.1007/978-3-319-59129-2_9

1 Introduction

The analysis of bone micro-architecture from 3D medical imaging techniques is of medical interest due to the clinical importance of osteoporosis [7]. For this purpose, high resolution peripheral quantitative computed tomography (HR-pQCT), micro computed tomography (micro-CT), cone beam computed tomography (CBCT), multi-slice computed tomography (MSCT), and magnetic resonance imaging (MRI) have been considered [8,9,15,19]. Among these, micro-CT is usually considered as the gold standard in preclinical studies thanks to its high resolution and contrast. However, micro-CT cannot be used in clinical settings, since it requires a high radiation dose [3]. For quantification, the computation of histomorphometric parameters plays a very important role [1]. Usually, these parameters are calculated from a binary image after segmenting trabecular bone from the background (bone marrow). Thus, the choice of a segmentation method may play an important role in structure measurements, but little attention is generally given to this fact [10].

Due to the variability in medical imaging techniques, there is no segmentation method that is ideal for all types of bone images. In histology images from prepared specimens, with high contrast and extremely high resolution, a simple thresholding is often sufficient for segmentation. In micro-CT, the resolution is usually high enough for such a simple approach. Unfortunately, for imaging methods applicable in vivo, such as CBCT and HR-pQCT, segmentation methods are more prone to errors. The most common segmentation methods for CT data are either based on adaptive or on double thresholding [2]. Similarly, Engelke et al. [5] have used thresholding based on the neighboring pixels in the micro-CT images of bone obtained through dual-energy CT. In our group, Petersson et al. [14] evaluated bone microstructure from clinical CT using the Automated Region Growing (ARG) algorithm [16].

CBCT is a 3D imaging modality that can be used in vivo, which might be considered for diagnosing bone-related diseases. The wide accessibility of the machines, the radiation dose, cost-effectiveness, and short scanning time, make this scanners appealing for evaluating the trabecular bone structure in clinical settings [17]. Still, trabecular bone characterization with CBCT has not yet been properly investigated, in particular when it comes to the importance of the selection of the segmentation method. In this study, we propose a new segmentation method based on granulometry, a concept from mathematical morphology that allows us to estimate thickness at a local scale [12]. The method is tested on CBCT data, using micro-CT images as a reference.

2 Segmentation Using Granulometries

In [12], we showed that granulometry in binary mathematical morphology is equivalent to the sphere-fitting method proposed in [6] for computing trabecular bone thickness. Such equivalence allowed us to create a method for estimating trabecular thickness on gray scale image data by replacing binary with gray

scale mathematical morphology. In this paper, we show that the method can be adapted to generate the segmentation of the image that can be used for extracting additional histomorphometric parameters.

The theory of granulometries was originally introduced by Matheron [11] to compute size distributions of grains in digital images. Intuitively, granulometry is analog to sieving the image with filters that emulate sieves of different hole sizes, where the size of a grain is determined by the minimum size of the hole that sifts the grain. A detailed mathematical description is found in [12].

The main procedure for computing trabecular thickness in gray scale is as follows. First, a granulometry is generated by applying the opening operation of mathematical morphology to the image with spherical structuring elements of different sizes E_1, E_2, ..., E_n. The openings are given by:

$$O_i = I \circ E_i = (I \ominus E_i) \oplus E_i, \tag{1}$$

where I is the image, $\ominus$ and $\oplus$ are the erosion and dilation morphological operations respectively. The thickness at a specific location x is related to the scale where the maximum change between consecutive openings is attained:

$$Th(x) = 2 \arg\max_t (O_t(x) - O_{t-1}(x)). \tag{2}$$

This procedure can be applied using binary or gray scale mathematical morphology. In [12], we discussed implementation issues that have to be considered for accurate estimation of thickness.

In an ideal noiseless scenario, using structuring elements E_i of sizes larger than the thickest trabecula will not have any effect on the results. Indeed, opening a noiseless image with a big enough structuring element will result in an image where all voxels have an intensity value of zero. However, this is not the case for noisy images. Thus, for efficiency purposes, it is necessary to stop the computation of openings at a scale larger than the thickest expected trabecula in the image. In the experiments on CBCT, considering that the thickest trabecula is expected to be of around 1 mm, we stopped the computations at scale 10, which corresponds to 1.5 mm.

The main effect of the opening operation on the image is that the gray scale dynamic range of values is reduced. Thus, the main hypothesis of our segmentation method is that after the final opening with E_n, the gray scale at trabecular bone is largely reduced compared to that reduction at bone marrow. The pipeline of the method is shown in Fig. 1.

The difference between the original and the last opening operation (cf. Fig. 1C) is higher in trabecular bone than in marrow. Since the contrast to noise ratio of this image is enhanced, a threshold can be used to get a final segmentation (cf. Fig. 1D). Thus the segmented image is computed as:

$$S = T(I - (I \circ E_n)) \oslash I, Th), \tag{3}$$

where I is the CBCT 3D image, S is the segmented image, E_n is the largest structuring element used for computing thickness, $\oslash$ is the Hadamard division

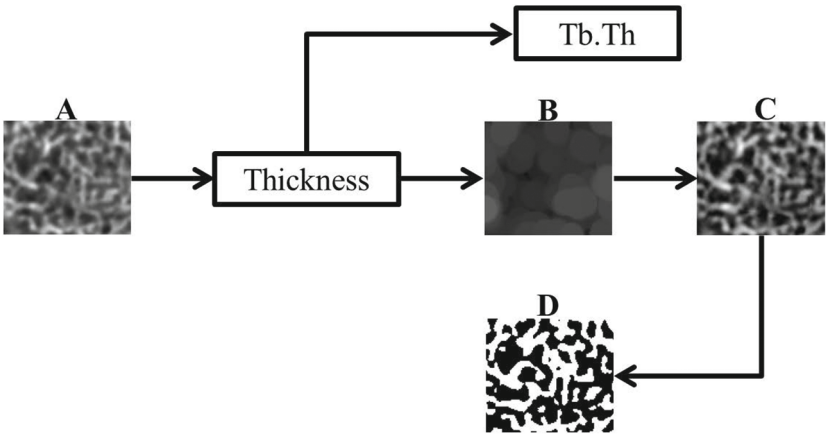

Fig. 1. Segmentation steps for the proposed method. A: original image, B: output of the last opening operation (residual), C: percentage of local gray scale reduction, D: final result after thresholding.

and T performs the threshold with Th. Although Th can be estimated adaptively using Otsu's threshold [13], we obtained good results with a fixed one (0.16) for our CBCT data in the experiments of Sect. 4.

3 Experimental Evaluation

We have studied our proposed granulometry-based segmentation technique on 14 human radius specimens [7]. The samples were donated for medical research in accordance with the ethical recommendations at the University of California, San Francisco. The specimens are almost cubic with a side of 12 to 15 mm and all include slabs of cortical bone, facilitating orientation. Two imaging techniques have been used in this study (Fig. 2):

- CBCT 3D images were acquired using the NewTom 5G (QR Verona, Verona, Italy) using a peak tube voltage of 110 kV, a tube current of 4.2–4.6 mA, and a field of view of 60 mm. After initial reconstruction with an isotropic resolution of 125 μm, the image was resampled by the scanner software to an isotropic voxel size of 75 μm.
- Micro-CT data were acquired with the Skyscan 1176 (Bruker micro-CT, Kontich Belgium) with a tube voltage of 65 kV, a tube current of 385 μA and an isotropic resolution of 8.67 μm.

The parameters were measured and calculated using MATLAB (MathWorks, Natick, MA). The code was developed in-house and calculated on a personal computer (PC) with Intel Core i7 (Intel Santa Clara, CA) at 2.60 GHz, 32 GB random access memory (RAM) and 64-bit operating system. We have compared

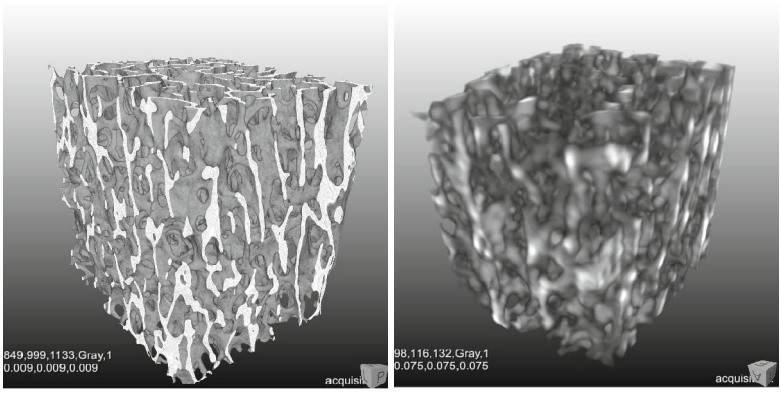

(a) (b)

Fig. 2. 3D view (a) MicroCT and (b) CBCT.

our algorithm with the Automatic Region Growing (ARG) algorithm [16] and Otsu's threshold [13], in the following referred to as Otsu.

Segmenting micro-CT data is not an issue thanks to its high resolution and contrast. Thus, in general, all segmentation methods perform well for micro-CT, including a basic thresholding. In this study, the micro-CT data were segmented with Otsu in order to avoid the use of parameters. We have studied six histomorphometric parameters: trabecular node density (Tb.Nd), trabecular termini density (Tb.Tm), trabecular separation (Tb.Sp), trabecular number (Tb.N), trabecular thickness (Tb.Th), and bone volume over total volume (BV/TV). The details of these parameters are given in [1]. These parameters were computed in 3D.

4 Results

Figure 3 shows qualitative results in the form of selected slices from CBCT. Judging from these images, Otsu and ARG segmentation algorithms give visually similar results. It is observed that granulometry-based segmentation gives results that are visually similar to those of ARG. In order to assess these differences, we measured the pairwise spatial overlap using the Dice coefficients [4]. The Dice coefficients between Otsu - ARG, Otsu - Granulometry and ARG - Granulometry are 0.9784, 0.8793 and 0.8763 respectively, which confirms the visual assessment.

Table 1 shows the value of the mean and standard deviation of the histomorphometric parameters extracted from the binary images obtained from different segmentation techniques. This table also includes the Tb.Th computed in gray scale as we proposed in [12]. As shown, both BV/TV and Tb.Th were overestimated by approximately 4 times. However, Tb.Sp and Tb.N were underestimated by a small amount. On the other hand, Tb.Nd and Tb.Tm were highly underestimated. We think this finding can be explained by spurious branches generated by the used skeletonization algorithm [18] on the micro-CT data. Moreover, these

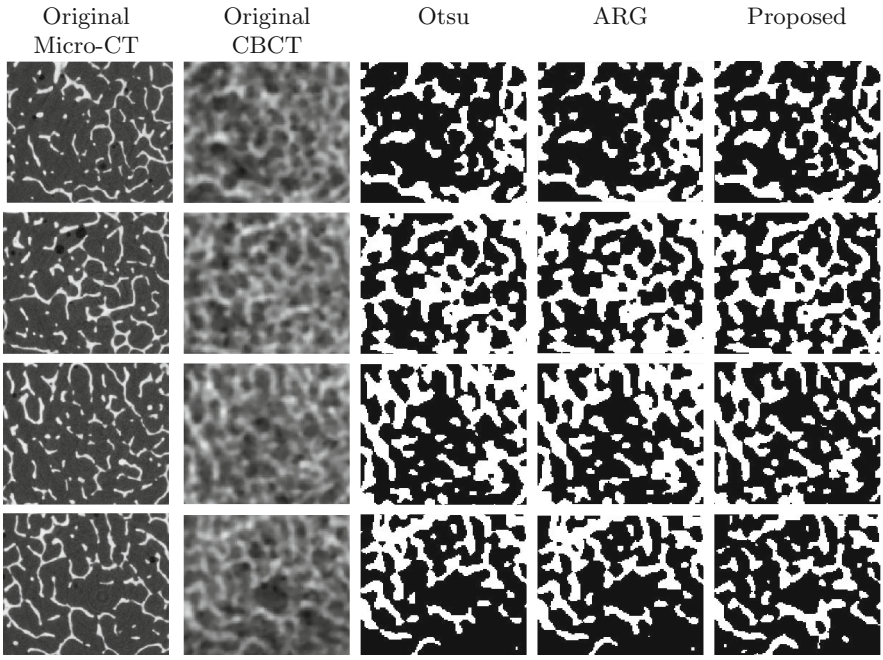

Fig. 3. Visual Segmentation Results using Otsu, ARG and Granulometry (proposed) for some selected slices.

parameters reflect the connectivity/topology of the network. The estimation of Tb.Th in gray scale is largely overestimated in this dataset.

In order to assess the performance of the proposed method, we computed the Pearson correlation coefficient of different parameters in Table 2, considering micro-CT images segmented with Otsu as our reference model.

Table 2 also reports the 95% confidence intervals for these differences. If a confidence interval does not include zero, the corresponding difference is statistically significant. As shown, for four parameters (Tb.Nd, Tb.N, Tb.Th and BV/TV), the proposed method reached larger correlations than 0.90, whereas Tb.Tm and Tb.Sp have correlations of 0.80 and 0.75, respectively. For three parameters (Tb.Nd, Tb.Tm and Tb.Sp), the strongest correlations with micro-CT images were found with ARG, and for three parameters with the new method (Tb.N, Tb.Th and BV/TV). As a way to compare the global performance of the methods, we computed the mean of the correlation coefficients. On average, our proposed granulometry-based segmentation yielded a correlation of 0.89 with micro-CT, which is stronger than for Otsu and ARG. Notice that the correlation between Tb.Th from micro-CT and Tb.Th in gray scale is the strongest. The reason of this is that this measurement is not affected by the segmentation algorithm and could be more appropriate for estimations in vivo. Unfortunately, except for Tb.Th, methods for estimating other parameters in gray scale are not currently available.

Table 1. Mean (± standard deviation) of different trabecular bone parameters.

Machine/ Segmentation	Tb.Nd (mm^{-3})	Tb.Tm (mm^{-3})	Tb.Sp (mm)	Tb.N (mm^{-1})	Tb.Th (mm)	BV/TV
CBCT/ARG	1.77±0.27	1.75±0.18	0.54±0.04	1.03±0.07	0.40±0.03	0.37±0.05
CBCT/ Otsu	2.66±0.65	1.68±0.42	0.46±0.09	1.31±0.21	0.25±0.02	0.24±0.04
CBCT/Granulometry	1.84±0.27	1.82±0.27	0.53±0.05	1.01±0.07	0.45±0.04	0.46±0.09
CBCT/No segmentation	-	-	-	-	0.82±0.25	-
Micro-CT/Otsu	58.5±15.6	86.3±21.9	0.68±0.10	1.37±0.18	0.13±0.01	0.10±0.02

Table 2. Pearson correlation coefficient between parameters computed on CBCT using micro-CT data segmented with Otsu as a reference. The 95% confidence limits are indicated in parenthesis. The strongest correlation for each parameter is highlighted in bold.

Segmentation	Tb.Nd	Tb.Tm	Tb.Sp	Tb.N	Tb.Th	BV/TV	Mean
Otsu	0.49 (0.00,0.79)	−0.07 (−0.55,0.43)	0.59 (0.13,0.83)	0.29 (−0.24,0.68)	0.89 (0.69,0.96)	0.59 (0.13,0.84)	0.45
ARG	**0.93** (0.81,0.97)	**0.81** (0.53,0.93)	**0.77** (0.45,0.91)	0.93 (0.80,0.97)	0.86 (0.64,0.95)	0.92 (0.76,0.97)	0.87
Granulometry	0.91 (0.76,0.97)	0.80 (0.49,0.92)	0.75 (0.40,0.90)	**0.97** (0.90,0.98)	0.91 (0.75,0.96)	**0.94** (0.83,0.97)	**0.89**
No segment	-	-	-	-	**0.97** (0.90,0.98)	-	-

5 Discussion

This paper has presented a method that uses the differences between the original and the residual images after granulometry analysis to increase the contrast of images acquired through CBCT. Such increase allowed us to use a threshold to segment the images.

The accuracy of the method was tested by comparing histomorphometric parameters computed in CBCT with respect to the ones obtained by micro-CT. Although gross systematic errors of the measurements on CBCT were found, the correlations were high for ARG and the proposed method. The proposed method yielded slightly better correlations compared to ARG.

Notice that the large systematic errors are more related to the low resolution and contrast of the CBCT images rather than to the segmentation algorithms. There are two strategies for handling these large systematic errors: (a) correct them using linear regression in order to give closer results to micro-CT or (b) use them as surrogates of the parameters estimated from micro-CT. In both cases, the measurements could be used for follow-up of treatments due to the strong correlations with micro-CT.

It is important to point out that, unlike ARG, the proposed method also estimates Tb.Th in gray scale. We found that such estimation of Tb.Th had the

strongest correlation to micro-CT data, suggesting that it is advantageous to compute histomorphometric parameters that do not require segmentation.

The method is especially useful for images acquired with modalities that can be used in vivo, such as CBCT, MSCT and HR-pQCT, where noise, resolution and contrast are relevant issues. Our ongoing research includes testing this method in these modalities. While the method can also be applied to micro-CT, the result is not different to the one from less elaborate strategies such as Otsu, due to the high resolution and contrast of these images. Moreover, the proposed method can be used for computing the Tb.Th in gray scale as well as for performing the segmentation at the same time, something that is not possible with ARG or Otsu. In this study, we used the skeletonization method proposed in [18] for performing the analysis of segmented images both in micro-CT and CBCT. We plan to test other skeletonization methods in order to assess the sensitivity of the estimations of histomorphometric parameters with respect to the skeletonization method.

To summarize, the results from this paper suggest that the combination of CBCT and granulometry-based segmentation can be used for monitoring changes in the microarchitecture of trabecular bone in a clinical environment. From the results of this study, we argue that our granulometry-based technique seems more promising than ARG for CBCT data. A limitation of the present study is the low number of specimens available. In the future, we will apply the method to larger CBCT materials as well as to HR-pQCT data.

Acknowledgments. This research has been supported by Eurostars, grant no. E9126, and by the Swedish Council for Research (VR), grants no- 2012-3512 and 2014-6153. The authors are grateful to Britt-Marie Andersson at Uppsala University for performing the micro-CT imaging and to Sharmila Majumdar at University of California for kindly providing the specimens. Per-Magnus Johansson at Maxillofacial radiology in Växjö helped us with the NewTom 5G imaging.

References

1. Bouxsein, M.L., Boyd, S.K., Christiansen, B.A., Guldberg, R.E., Jepsen, K.J., Müller, R.: Guidelines for assessment of bone microstructure in rodents using micro-computed tomography. J. Bone Min. Res. **25**(7), 1468–1486 (2010)
2. Chevalier, F., Laval-Jeantet, A., Laval-Jeantet, M., Bergot, C.: CT image analysis of the vertebral trabecular network in vivo. Calcif. Tissue Int. **51**(1), 8–13 (1992)
3. Christiansen, B.A.: Effect of micro-computed tomography voxel size and segmentation method on trabecular bone microstructure measures in mice. Bone Rep. **5**, 136–140 (2016)
4. Dice, L.R.: Measures of the amount of ecologic association between species. Ecology **26**, 297–302 (1945)
5. Engelke, K., Graeff, W., Meiss, L., Hahn, M., Delling, G.: High spatial resolution imaging of bone mineral using computed microtomography: comparison with microradiography and undecalcified histologic sections. Invest. Radiol. **28**(4), 341–349 (1993)

6. Hildebrand, T., Rüegsegger, P.: A new method for the model-independent assessment of thickness in three-dimensional images. J. Microsc. **185**(1), 67–75 (1997)
7. Klintström, E., Klintström, B., Moreno, R., Brismar, T.B., Pahr, D.H., Smedby, Ö.: Predicting trabecular bone stiffness from clinical cone-beam CT and HR-pQCT data; an in vitro study using finite element analysis. PloS ONE **11**(8), e0161101 (2016)
8. Laib, A., Rüegsegger, P.: Comparison of structure extraction methods for in vivo trabecular bone measurements. Comput. Med. Imaging Graph. **23**(2), 69–74 (1999)
9. Majumdar, S., Gies, A., Newitt, D., Osman, D., Chiu, E., Truong, V., Genant, H., Lotz, J., Kinney, J.: Assessment of trabecular bone structure using magnetic resonance imaging and X-ray tomographic microscopy. Osteoporos. Int. **6**, 376–385 (1996)
10. Majumdar, S., Newitt, D., Jergas, M., Gies, A., Chiu, E., Osman, D., Keltner, J., Keyak, K., Genant, H.: Evaluation of technical factors affecting the quantification of trabecular bone structure using magnetic resonance imaging. Bone **17**(4), 417–430 (1995)
11. Matheron, G.: Random Sets and Integral Geometry. Wiley, New York (1975)
12. Moreno, R., Borga, M., Smedby, Ö.: Estimation of trabecular thickness in gray-scale images through granulometric analysis. In: Proceedings of SPIE - Medical Imaging, vol. 8314, p. 831451 (2012)
13. Otsu, N.: Threshold selection method from gray-level histograms. IEEE Trans. Syst. Man Cybern. **9**(1), 62–66 (1979)
14. Petersson, J., Brismar, T., Smedby, Ö.: Analysis of skeletal microstructure with clinical multislice CT. In: Larsen, R., Nielsen, M., Sporring, J. (eds.) MICCAI 2006. LNCS, vol. 4191, pp. 880–887. Springer, Heidelberg (2006). doi:10.1007/11866763_108
15. Peyrin, F., Houssard, J.P., Maurincomme, E., Peix, G., Goutte, R., Laval-Jeantet, A.M., Amiel, M.: 3D display of high resolution vertebral structure images. Comput. Med. Imaging Graph. **17**(4–5), 251–256 (1993)
16. Revol-Muller, C., Peyrin, F., Carrillon, Y., Odet, C.: Automated 3D region growing algorithm based on an assessment function. Pattern Recogn. Lett. **23**(1–3), 137–150 (2002)
17. Van Dessel, J., Huang, Y., Depypere, M., Rubira-Bullen, I., Maes, F., Jacobs, R.: A comparative evaluation of cone beam CT and micro-CT on trabecular bone structures in the human mandible. Dentomaxillofacial Radiol. **42**(8), 20130145 (2013)
18. Xie, W., Thompson, R.P., Perucchio, R.: A topology-preserving parallel 3D thinning algorithm for extracting the curve skeleton. Pattern Recogn. **36**(7), 1529–1544 (2003)
19. Zhou, B., Wang, J., Yu, Y.E., Zhang, Z., Nawathe, S., Nishiyama, K.K., Rosete, F.R., Keaveny, T.M., Shane, E., Guo, X.E.: High-resolution peripheral quantitative computed tomography (HR-pQCT) can assess microstructural and biomechanical properties of both human distal radius and tibia: ex vivo computational and experimental validations. Bone **86**, 58–67 (2016)